Available online at www.sciencedirect.com
ScienceDirect
Wear 265 (2008) 1–7
WEAR
www.elsevier.com/locate/wear

Development of wear resistant carbidic austempered ductile iron (CADI)

S. Laino, J.A. Sikora, R.C. Dommarco *

Grupo Tribología - Facultad de Ingeniería, División Metalurgia - INTEMA, Universidad Nacional de Mar del Plata - CONICET, Av. J.B. Justo 4302, B7608FDQ Mar del Plata, Argentina

Received 2 June 2006; received in revised form 15 June 2007; accepted 21 August 2007
Available online 29 October 2007

Abstract

The abrasion wear resistance of irons may be improved by the incorporation of an extra phase to the matrix, typically consistent of carbides. Nevertheless, the improvement in wear resistance is generally accompanied by a decrease in the impact toughness. The aim of this work is to study the methodology to obtain a controlled precipitation of carbides in a ductile cast iron that is subsequently austempered, obtaining the so-called carbidic austempered ductile iron (CADI). This material is expected to offer high abrasion resistance but still retaining higher impact toughness than other reinforced irons, thanks to the particular characteristics of the matrix. A plate model with a copper chill allowed to evaluate both, the influence of a high cooling rate and the effect of alloying elements on carbide precipitation. Four different alloys with equivalent carbon close to the eutectic composition were used in order to evaluate the effect of chromium contents ranging from 1 to 2.5%. A detailed microstructural characterisation of the material was made, studying particularly carbide content and composition, besides their stability during the heat treatment. The abrasion wear resistance was evaluated by testing under the ASTM G 65 standard, obtaining relative wear resistance values ranging between 1.02 and 1.95 with respect to conventional ADI samples taken as reference material. The impact toughness decreased from about 138–101 J for ADI to about 26–7 J for CADI.

Keywords: Carbidic austempered ductile iron; Microstructure; Carbides; Abrasion; Impact toughness

1. Introduction

Austempered Ductile Iron (ADI) has been long recognised for its high tensile strength and toughness (over 1600 MPa and over 100 J for grades 5 and 1, respectively, according to the ASTM A 834-95), making possible to replace forged steels in many applications. It is also well known the ability of this material to perform very well under different wear mechanisms such as rolling contact fatigue, adhesion and abrasion [1–3].

ADI has proved to behave in a different manner under abrasive conditions, depending on the tribosystem (low or high stress abrasion), but being always possible to obtain a good performance in service if the heat treating parameters are properly selected [2].

A new type of ADI, containing carbides immersed in the typical ausferritic matrix, called carbidic ADI or CADI has been recently introduced in the market. Nevertheless, the literature available only show application examples and data about the response to abrasive wear but not the procedure to produce CADI.

The presence of carbides is expected to promote an increase in the abrasion wear resistance, but on the other hand toughness is expected to decrease. Therefore, the challenge related to the development of this material is to be able to control the microstructure in order to obtain the optimum balance between abrasion resistance and toughness, taking into account the tribosystem and the operating conditions.

One of the methodologies commonly used to obtain a microstructure with as-cast carbides is to reduce the quantity of graphitising elements (in particular Si), in order to promote the precipitation of ledeburitic carbides during solidification due to a closer interval between the stable and metastable diagrams. This methodology may be combined with a second option given by the high undercooling promoted by the use of a chill in the mould. A third option is to alloy the melt with carbide stabilising elements, such as chromium, molybdenum or titanium [4,5], which strongly reduce the interval between stable and metastable eutectic temperatures and promote total or partial solidification

* Corresponding author.
E-mail address: dommarco@fi.mdp.edu.ar (R.C. Dommarco).

0043-1648/$ – see front matter © 2007 Elsevier B.V. All rights reserved.
doi:10.1016/j.wear.2007.08.013

according to the metastable diagram [6]. It must be taken into account that an undercooling also affects the size and count of the solidification units, and therefore, the microsegregation. The lower the cooling rate, the greater the microsegregation effect increasing the probability for carbide precipitation at the last to freeze zones, and therefore, the formation of alloyed carbides. Then, the size and composition of carbides may vary, from typical unalloyed ledeburitic to thin plate shaped high-alloyed carbides, depending on the chemical composition and cooling rate [6–9].

It was demonstrated [10] that ledeburitic carbides produced either by controlling the cooling rate or the silicon level (non-alloyed carbides) have a high tendency to dissolve during the austenitizing stage and are less stable than alloyed carbides. Therefore, carbide dissolution during heat treatment should be evaluated.

The objectives of this work is to produce different variants of CADI, studying its microstructural characteristics and evaluating some mechanical properties, particularly the abrasion resistance and the impact toughness.

2. Experimental procedure

2.1. Sample preparation

The material used in this study was obtained in a metal casting laboratory, using a 55 kg capacity 3 kHz induction furnace. Steel scrap and foundry returns were used as charge materials. In all cases the melts were nodulized with FeSiMg (9 wt.% Mg) and inoculated with FeSi (75 wt.% Si). Five alloys of ductile iron were obtained, with approximately 0, 1.0, 1.5, 2.0 and 2.5 wt.% Cr.

The shape and dimensions of the model used [11,12] is shown in Fig. 1. A copper chill of 38 mm × 38 mm × 200 mm was positioned at the end of the plate in order to promote a chilling effect in its vicinity introducing a cooling rate gradient along the plate.

A numerical simulation of the feeding and solidification processes was carried out by using the software Nova Flow & Solids®. The simulation was used to evaluate the variation of the cooling rate with the distance to the chill and to determine the distance at which the chill is no longer effective.

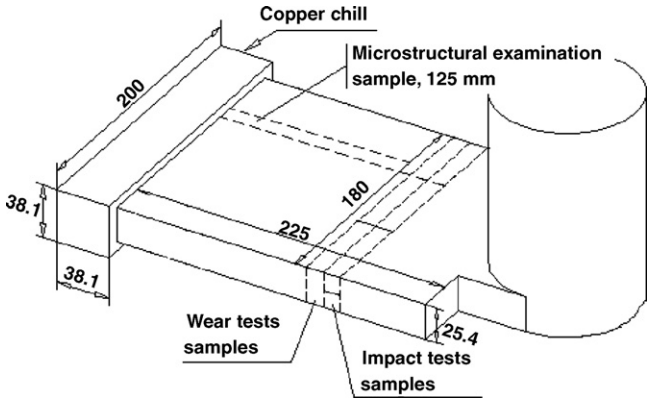

Fig. 1. Plate model with copper chill at one end showing the location where test samples were obtained.

Table 1
Sample identification, in both the as-cast and treated conditions

Identification	Heat (% Cr)	Condition	Austempering temperature (°C)
C1	1 (2.5)	As-cast	–
A1-280	1 (2.5)	Austempered	280
A1-360	1 (2.5)	Austempered	360
C2	2 (2.0)	As-cast	–
A2-280	2 (2.0)	Austempered	280
A2-360	2 (2.0)	Austempered	360
C3	3 (1.5)	As-cast	–
A3-280	3 (1.5)	Austempered	280
A3-360	3 (1.5)	Austempered	360
C4	4 (1.0)	As-cast	–
A4-280	4 (1.0)	Austempered	280
A4-360	4 (1.0)	Austempered	360
C5	5 (0)	As-cast	–
ADI 280	5 (0)	Austempered	280
ADI 360	5 (0)	Austempered	360

Austenitizing temperature 900 °C in all samples.

The plates were cut as shown in Fig. 1, with a longitudinal slice ∼125 mm long obtained for the microstructural characterisation, carbide quantification and dissolution studies. At distances between 125 and 150 mm (zone not affected by the chill), two slices ∼11 mm thick were cut (Fig. 1), from which impact and wear test samples were obtained. Hardness measurements were also performed on all samples.

The samples obtained from the five alloys were then heat treated by austenitizing 1 h at 900 °C in a muffle followed by an austempering step in a salt bath for 2 h, at two different temperatures, 280 and 360 °C. The unalloyed samples without carbides (conventional ADI) were used as reference material for wear and impact tests together with the CADI variants (having different carbide contents). Sample identification in both the as-cast and heat treated conditions is listed in Table 1.

2.2. Chemical and microstructural examination

The chemical composition of the alloys was determined by means of a Baird Spark Emission Optic Spectrometer with a DV6 excitation source. The chemical composition of the carbides was evaluated by using a Philips Scanning Electron Microscope with an EDX module, in order to analyse the microsegregation effects and its influence on the carbide dissolution during heat treatment. The values reported are the average of three determinations.

Metallographic sample preparation for optical microscopy examination was carried out by using standard techniques for cutting and polishing before etching with 2% Nital. In order to quantify the amount of carbides, they were revealed by etching with 10% ammonium persulfate in aqueous solution and its content (in percent) was measured in zones located every 2 mm starting from the chill by using the Image Pro Plus software. The magnification used was 50× in order to obtain data from a sufficiently large area. Each reported value is the average of three determinations.

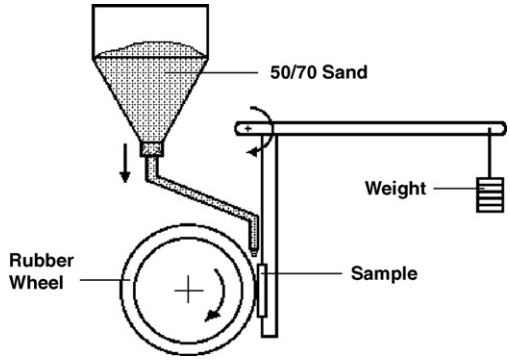

Fig. 2. Schematic of the ASTM G 65 dry sand–rubber wheel abrasion test.

2.3. Mechanical tests

The Brinell hardness (HBW) of the samples was measured using a 2.5 mm tungsten carbide ball and a bench tester with a load of 187.5 kg. Microindentation tests were carried out in order to determine the hardness of carbides by using a Vickers indenter and a 200 g load.

The abrasion wear resistance of the samples was evaluated by means of the "Dry Sand/Rubber Wheel Abrasion Test", Fig. 2, according to the ASTM G 65 standard and using the procedure A (specimen load 130 N, wheel revolutions 6000). The relative wear resistance index—E, was obtained by the relationship between the volume loss experienced by conventional ADI samples, used as reference materials (ΔV_R), and the CADI samples (ΔV_S), according to Eq. (1). The weight loss values were measured by means of a 0.1 mg precision scale and then converted into volume loss by using the material density measured on calibrated blocks made from all the alloys used in this study.

$$E = \frac{\Delta V_R}{\Delta V_S} \quad (1)$$

Impact toughness tests on ADI and CADI samples were carried out under the ASTM E 23 standard, using 10 mm × 10 mm × 55 mm specimens and an Amsler pendulum with an initial energy of 300 J (5 m/s impact speed). Due to the characteristics of the materials evaluated unnotched samples were used. The reported values are the average of two determinations.

3. Results and discussion

3.1. Cooling curves

The cooling curves as a function of the distance along the plate were evaluated, simulating the solidification process by finite element analysis under two conditions, with and without the chill. The values of the cooling rate were calculated as the slope of the curve at the start of the solidification process.

The cooling rate values at different distances from the chill (d) are listed in Table 2 and the results under the two conditions evaluated are compared, showing that the chill is not longer effective at distances greater than ~75 mm where the cooling rates stabilise at ~1.3 °C/s. These results were validated by the microstructural examination and were used in order to obtain samples from regions affected or not by the chill. The correlation between the cooling rates and the microstructure will also allow predicting the microstructure under different chill/part geometry and size combinations.

Table 2
Cooling rates at different zones of the plate, calculated from cooling curves simulated with and without the chill

Distance to chill (mm)	Cooling rate (°C/s) (with chill)	Cooling rate (°C/s) (without chill)
5	41.64	2.79
17	8.16	2.28
29	3.11	1.81
41	1.88	1.59
53	1.48	1.33
75	1.35	1.34
100	1.33	1.31
150	1.31	1.30

Nevertheless, the ideal CADI structure would be that obtained without the use of a chill, in order to facilitate or simplify the industrial process. Thus, in the present paper, the microstructure of chilled regions was evaluated, leaving the mechanical properties of this region for a future work. The samples for microstructural characterisation include regions affected and not affected by the chill, while the samples for hardness, wear and impact tests were only taken from regions not affected by the chill.

3.2. Chemical and microstructural characterisation

Table 3 lists the chemical composition of the different alloys, C1, C2, C3, C4 and C5, showing in all cases an approximately eutectic composition (equivalent carbon, EC ~4.3). As it was stated, the main alloying element was Cr, introduced in different amounts to promote carbide precipitation. Alloy C5 was not alloyed with Cr in order to obtain the base ductile iron used to produce the conventional ADI samples used as reference material. Cu and Ni were added in small quantities in order to increase the austemperability.

Figs. 3–6 show the microstructures of samples A1-280, A2-280, A3-280 and A4-280, respectively, at two different locations of the plates. Figs. 3–6a), show the microstructures at $d = 5$ mm having a high carbide concentration as well as a high nodule count with a small graphite nodule size (typically about 10–15 μm) due to the relatively high cooling rate. Figs. 3–6b) show the microstructures at $d = 100$ mm, where the cooling rate is lower than that present at $d = 5$ mm, and is not affected by the chill. At lower cooling rates, less amount of carbides

Table 3
Chemical composition for the different heats evaluated (wt. %)

Heat	C	Si	Mn	S	P	Cu	Ni	Cr	EC
C1	3.35	3.09	0.18	0.039	0.042	0.67	0.58	2.59	4.38
C2	3.40	3.00	0.13	0.015	0.039	0.65	0.56	2.04	4.40
C3	3.29	3.28	0.15	0.019	0.035	0.60	0.59	1.45	4.38
C4	3.18	3.38	0.13	0.016	0.037	0.63	0.61	0.84	4.31
C5	3.40	3.34	0.17	0.019	0.035	0.62	0.63	0	4.51

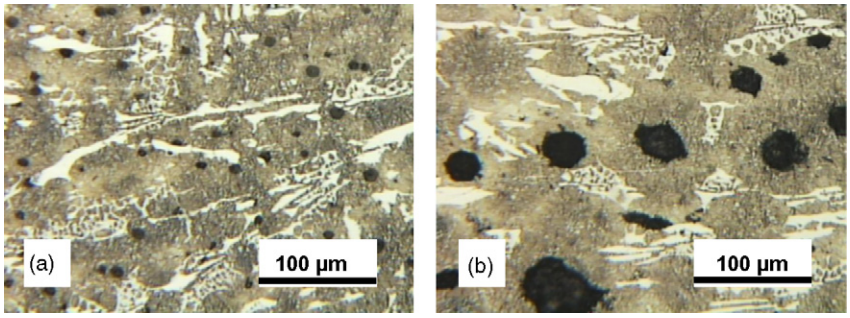

Fig. 3. Microstructures of sample A1-280 at (a) 2 mm and (b) 100 mm from the chill.

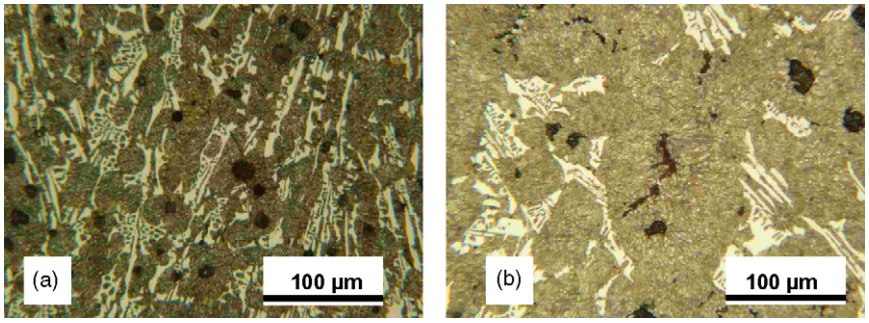

Fig. 4. Microstructures of sample A2-280 at (a) 2 mm and (b) 100 mm from the chill.

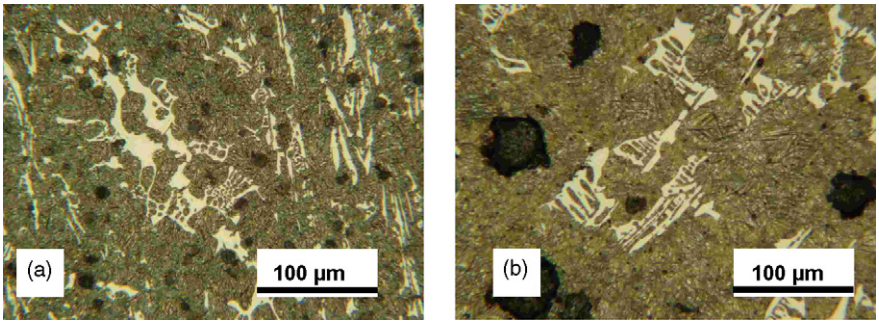

Fig. 5. Microstructures of sample A3-280 at (a) 2 mm and (b) 100 mm from the chill.

with larger size, and lower nodule count with higher graphite nodule size are observed. The matrix is fully ausferritic in all cases, showing the good austemperability of the different alloys.

The chromium contents of carbides present in alloys C1 and C4, determined by EDX, are listed in Table 4, showing that the carbides are of the type M_3C, with chromium partially substituting iron. Carbides alloyed with chromium contents of 5.9 and 2.8% were found at $d = 5$ mm for alloys C1 and C4 with global % Cr of 2.5 and 1.0, respectively. In the same alloys, at a higher distance ($d = 100$ mm) the lower cooling rate promote larger solidification units, and therefore, higher microsegrega-

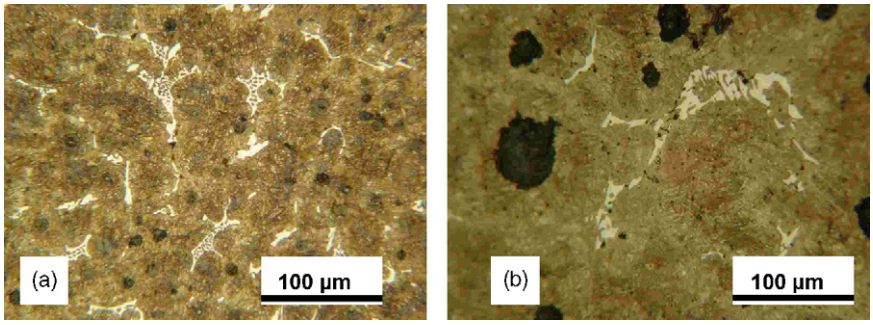

Fig. 6. Microstructures of sample A4-280 at (a) 2 mm and (b) 100 mm from the chill.

Table 4
Chromium content in carbides determined by EDX at different zones for heats C1 and C4

Material variant (global % Cr)	Chromium in each zone	
	$d = 5$ mm to chill	$d = 100$ mm to chill
C1 (2.5)	5.9%	8.2%
C4 (1.0)	2.8%	6.7%

tion effects, leading to an increase in the Cr content found in the carbides, 8.2 and 6.7% Cr for alloys C1 and C4, respectively.

Fig. 7 shows the carbide content versus the distance to the chill in both, the as-cast (samples C1, C2, C3 and C4) and the heat treated (samples A1, A2, A3 and A4) conditions. The maximum carbide content was about 30% for alloys C1 and C2 close to the chill, while the minimum was about 5% for alloy C4 at distances far away from the chill. The carbide content after the heat treatment remains mostly unchanged. The absence of carbide dissolution has been justified [10] by the high thermodynamic stability of alloyed carbides due to the high chromium content of the alloys (considering ductile irons production practice) and mainly the microsegregation effect, which is strongly evidenced in the last to freeze zones. It can also be observed in Fig. 7 that the influence of the cooling rate on carbide precipitation decreases as the chromium content decreases.

3.3. Mechanical properties

3.3.1. Hardness tests

The Brinell hardness was determined at $d > 100$ mm as the average of five determinations, with a maximum standard deviation $\sigma_{n-1} \approx 6.4$ for samples A1-280 and A2-280 and with $\sigma_{n-1} < 4$ for the remaining samples. The results for the two austempering temperatures are reported in Fig. 8, showing that the reinforcing effect of carbides increases with the carbide content following a trend similar to that obtained by using the equivalent hardness (lever rule) concept [13]. The reinforcing effect of carbides on hardness was very similar for the two austempering temperatures evaluated.

The Vickers microhardness of the carbides was determined as the average of three measurements in each alloy in a region located at $d > 100$ mm where larger carbides are present. Carbides hardness of about 1100 HV_{200} with a maximum dispersion $\sigma_{n-1} = 25$ were found in all samples.

3.3.2. Wear resistance

Fig. 9 shows the density values for all the alloys measured on 10 mm × 10 mm × 25 mm ground calibrated blocks. In order to validate the accuracy of the method used, the density of a SAE 1010 block was also measured and reported.

Tables 5 and 6 list the relative wear resistance (E) values obtained for all the CADI samples at the two austempering temperatures, 280 and 360 °C. The reported values are the average of four determinations, with a maximum $\sigma_{n-1} = 0.06$. In each case, the CADI samples were compared against the conventional ADI (0% Cr) austempered at the same temperature, i.e. ADI 280 and

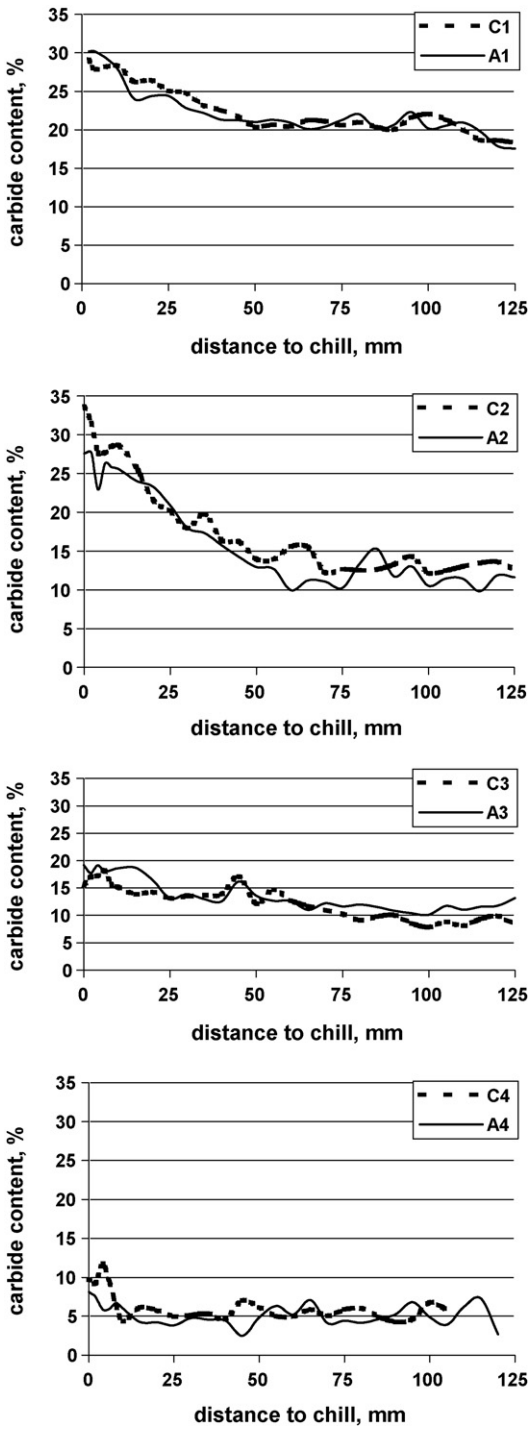

Fig. 7. Carbide contents (%) in as-cast (C1, C2, C3, C4) and austempered (A1, A2, A3, A4) samples.

Table 5
Relative wear resistance (E) values for CADI samples austempered at 280 °C; reference material, ADI 280

Sample (% Cr)	Relative wear resistance: E
ADI 280 (0)	1
A1-280 (2.5)	1.73
A2-280 (2.0)	1.52
A3-280 (1.5)	1.45
A4-280 (1.0)	1.23

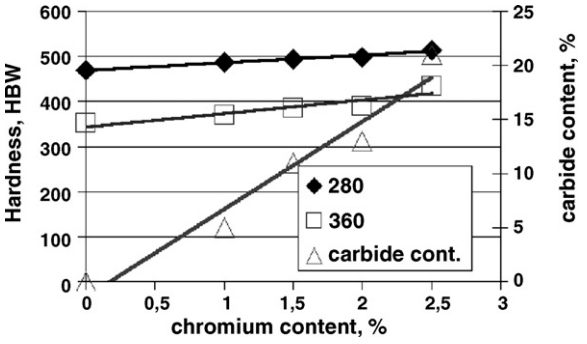

Fig. 8. Hardness (HBW) and carbide content values for all CADI variants versus chromium content.

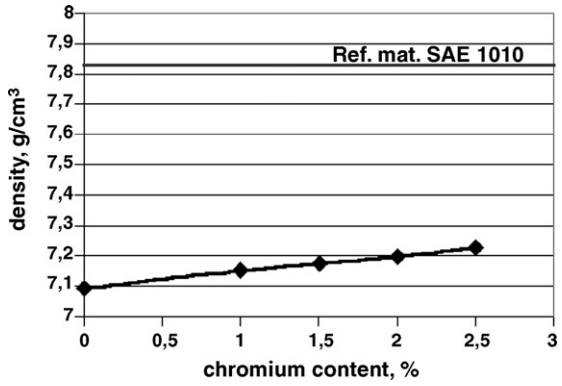

Fig. 9. Density values as a function of the chromium content for all heats evaluated.

ADI 360 samples were used as reference materials. These values show that the reinforcing effect of carbides was higher for the softer matrix (ADI 360). A similar response with respect to hardness was also observed in ADI austempered at different temperatures [2] and also tested by following the ASTM G 65 standard, even though, the same material variants behave differently under more severe abrasive conditions. These results are also presented in Fig. 10 in the form of volume loss as a function of chromium content, showing an important increase in the reinforcing effect of carbides when % Cr is 1.5% or higher.

3.3.3. Impact tests

The results of the impact toughness (J) versus chromium content in all the material variants studied are shown in Fig. 11. For an easier interpretation the carbide content is also shown besides the chromium content. As expected, the impact toughness decreased as the Cr or carbide contents increased, but

Table 6
Relative wear resistance (E) values for CADI samples austempered at 360 °C; reference material, ADI 360

Sample (% Cr)	Relative wear resistance: E
ADI 360 (0)	1
A1-360 (2.5)	1.95
A2-360 (2.0)	1.76
A3-360 (1.5)	1.6
A4-360 (1.0)	1.08

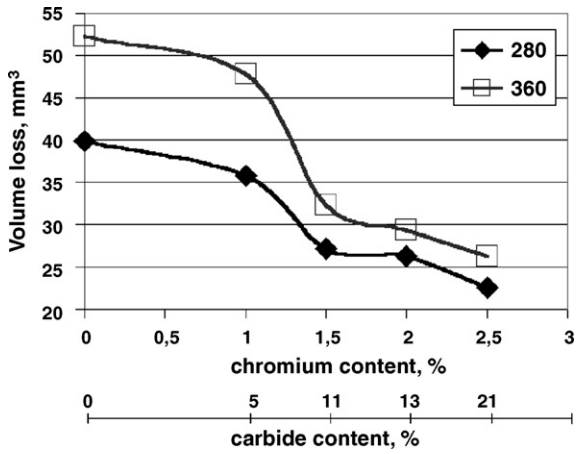

Fig. 10. Volume loss values as a function of the chromium content for samples austempered at 280 and 360 °C. (procedure, ASTM G 65 standard).

reaching a cuasy-steady level at ~7 J for a % Cr > 1.5 for the two austempering temperatures. In order to compare with CADI samples, conventional ADI 280 and ADI 360 were also evaluated obtaining impact toughness values of 101 and 138 J, respectively. The maximum standard deviation was $\sigma_n = 2.4$ for the CADI samples and $\sigma_n = 16.2$ for the reference conventional ADI samples. There was also an influence of the ausferritic matrix in the impact toughness. For all the Cr contents the samples austempered at 360 °C have higher toughness than those austempered at 280 °C, since the feathery microstructure of the former have higher ability to deform than the acicular microstructure of the later.

The analysis of the wear tests and the impact toughness results are also reported in Table 7 showing that the alloy with 1.5% Cr (A3-280 and A3-360) and also alloys A2-360 (2% Cr) and A4-280 (1% Cr) have a good balance between wear resistance and impact toughness, under the current experimental conditions. These material variants have shown an important improvement in abrasion resistance with respect to the ADI variants, while at the same time show good impact toughness when compared to alloys with higher Cr content. Nevertheless, for in service applications (different tribosystems) additional or different considerations could be needed.

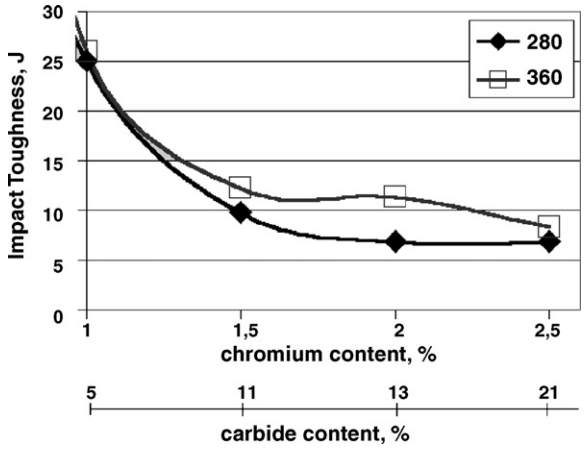

Fig. 11. Impact toughness versus chromium content for ADI and CADI samples.

Table 7
Ranking of wear resistance for all the samples evaluated, besides the impact toughness for each variant

Sample	Volume loss (mm^3)	Impact toughness (J)
A1-280	23.29	6.8
A2-280	26.57	6.8
A1-360	27.14	8.3
A3-280	27.86	9.8
A2-360	30.14	11.3
A4-280	32.71	25
A3-360	33.14	12.2
ADI 280	40.29	101.5
A4-360	48.86	26
ADI 360	52.86	138

4. Applications of CADI in real parts

Under ideal conditions, the use of a material for a new application should be evaluated through field tests, even with their associated difficulties such as higher cost, sample tracking, machine shut downs, etc.

The performance of wheel loader bucket protection plates made of CADI containing 1.0 and 2.0% Cr and austempered at 300 °C is currently being assessed by field tests, using a conventional ADI also austempered at 300 °C as reference material. This type of solicitation was deliberately chosen in order to get abrasive conditions different to that evaluated in the lab.

5. Conclusions

It has been possible to obtain carbidic ADI (CADI) with different amount of carbides using Cr as the main alloying element. The carbide contents for Cr between 1 and 2.5% were in the range of 5–21%. Most carbides were stable during the austenitizing stage of the austempering and the amount of dissolved carbides was very low or negligible.

The presence of carbides in the microstructure may increase the wear resistance by up to 100% with respect to a conventional ADI austempered at the same temperature. Under the present experimental conditions the presence of carbides in the alloys containing 1.5% Cr or more produced a significant reinforcement of the matrix with respect to abrasion.

As expected, the impact toughness decreased with the amount of chromium, but reaching a cuasy-steady level at ∼7 J for a % Cr > 1.5 for the two austempering temperatures investigated. Alloys containing 1% Cr showed higher values of impact toughness (∼25 J). Under the current experimental conditions the highest wear resistance was obtained for sample A1-280, with the highest chromium content (2.5% Cr) and the lowest austempering temperature (280 °C). Nevertheless, when impact toughness needs to be taken into account other material variants should be looked at. For the two austempering temperatures evaluated the alloy with 1.5% Cr (samples A3-280 and A3-360) and also the alloys with 2.0% Cr (samples A2-360) and 1% Cr (samples A4-280) showed very good balance between wear resistance and impact toughness.

The performance of wheel loader bucket protection plates made of CADI is currently being assessed by field tests in order to get the material response under different abrasive conditions.

References

[1] L. Magalhães, J. Seabra, Wear and scuffing of austempered ductile iron gears, Wear 215 (1998) 237–246.
[2] R. Dommarco, I. Galarreta, H. Ortiz, P. David, G. Maglieri, The use of ductile iron for wheel loader bucket tips, Wear 249 (2001) 101–108.
[3] R. Dommarco, J. Salvande, Contact fatigue resistance of austempered and partially chilled ductile irons, Wear 254 (2003) 230–236.
[4] J.R. Keough, K.L. Hayrynen, Carbidic austempered ductile iron (CADI), Ductile Iron News 3 (2000).
[5] K.L. Hayrynen, K.R. Brandenberg, Carbidic austempered ductile iron (CADI)—the new wear material, Am. Foundry Soc. 111 (2003) 845–850.
[6] R.B. Gundlach, J.F. Janowak, S. Bechet, K. Rohrig, On the problems with carbide formation in gray cast iron, in: Materials Research Society Symposium Proceedings, 34, 1985, pp. 251–261.
[7] J. Lacaze, G. Torres Camacho, C. Bak, Microsegregation in mottled spheroidal graphite cast iron, Int. J. Cast Met. Res. 16 (2003) 167–172.
[8] L. Nastac, D.M. Stefanescu, Modeling of the stable-to-metastable structural transition in cast iron, Adv. Mater. Res. 4–5 (1997) 469–478.
[9] H. Zhao, B. Liu, Modeling of stable and metastable eutectic transformation of spheroidal graphite iron casting, ISIJ Int. 41 (2001) 986–991.
[10] M. Caldera, G. Rivera, R. Boeri, J. Sikora, Precipitation and dissolution of carbides in low alloy ductile iron plates of varied thickness, Mater. Sci. Technol. 21 (10) (2005) 1187–1191.
[11] J. Hemanth, Fracture toughness of austempered chilled ductile iron, Mater. Sci. Technol. 15 (1999) 878–884.
[12] J. Hemanth, Wear characteristics of austempered chilled ductile iron, Mater. Des. 21 (2000) 139–148.
[13] K.S. Al-Rubaie, Equivalent hardness concept and two-body abrasion of iron-base alloys, Wear 243 (2000) 92–100.